Morphometric descriptive report of scleral ossicle rings, by ultrasound and computed tomography, in three Testudines specimens

Stelamares Boyda de Andrade[1,2] Nayone Lima Lantyer Cordeiro de Araujo[2]
Ana Cláudia Santos Raposo[2] Caterina Muramoto[2] Arianne Pontes Oriá[2*]

[1]Universidade Federal do Oeste da Bahia (UFOB), Centro Multidisciplinar Campus Barra (CMB), Barra, BA, Brasil.
[2]Escola de Medicina Veterinária e Zootecnia (EMEVZ), Departamento de Anatomia, Patologia e Clínicas Veterinárias, Universidade Federal da Bahia (UFBA), 40170-110, Salvador, BA, Brasil. E-mail: arianneoria@ufba.br. *Corresponding author.

ABSTRACT: *The scleral ossicle rings function has been related to mechanical protection, muscle fixation, support for eyeball shape and visual accommodation. There are few morphobiometric reports on these rings in different Testudines species, and we performed ultrasound (US) and computed tomography (CT) of the scleral ossicle rings in one green turtle (Chelonia mydas), one black-bellied slider (Trachemys dorbigni) and one red-footed tortoise (Chelonoidis carbonarius). The US and CT of the ossicle rings were performed for anatomical identification. The thickness, density, width, and diameters of each ring were measured. The US and CT of the scleral ossicle rings of three animals showed single and continuous circular structures, located in the anterior pole. These structures were easily observed in C. mydas, whose rings were the biggest, thickest and widest. The T. dorbigni CT presented decreased dimensions and the ossicles were the most difficult to identify. Bone density in the superior region was greater than in the inferior of each ring in all animals. Non-invasive imaging exams are good tools to study the anatomy of the ocular skeleton. The scleral ossicle rings of the three specimens presented general morphological similarities and CT enabled visualizing a greater number of details of the ring bone morphology.*
Key words: *chelonian, eye morphology, image, ocular skeleton, scleral ossicles.*

Relato descritivo morfobiométrico dos anéis de ossículos esclerais, por ultrassonografia e tomografia computadorizada, em três espécimes de Testudines

RESUMO: *Os anéis de ossículos esclerais têm sua função relacionada à proteção mecânica, fixação muscular, suporte para o formato do bulbo ocular e acomodação visual, contudo existem poucos relatos morfobiométricos sobre esses anéis em diferentes espécies de Testudines. Desta forma, foi realizada a avaliação morfobiométrica, por ultrassom (US) e tomografia computadorizada (TC), dos anéis de ossículos esclerais em uma tartaruga verde (Chelonia mydas), um tigre-d'água (Trachemys dorbigni) e um jabuti-piranga (Chelonoidis carbonarius). Foram realizadas US e TC dos anéis esclerais dos três animais para identificação anatômica, espessura, densidade, largura e diâmetros. A US e a TC dos três animais mostraram estruturas circulares únicas e contínuas, localizadas no polo anterior. Estas estruturas foram facilmente observadas na C. mydas, cujos anéis eram os maiores, mais espessos e mais largos. A TC da T. dorbigni apresentou dimensões reduzidas e os ossículos foram dificilmente identificados. A densidade óssea na região superior foi maior comparativamente a parte inferior de cada anel, em todos os animais. Exames de imagem não invasivos mostraram-se bons instrumentos para estudo do esqueleto escleral. Os anéis de ossículos esclerais dos três espécimes apresentaram semelhanças morfológicas gerais e a TC permitiu visualizar um maior número de detalhes da morfologia óssea do anel.*
Palavras-chave: *esqueleto ocular, imagem, morfologia ocular, ossículos esclerais, quelônios.*

INTRODUCTION

Green turtle (*Chelonia mydas*)*,* black-bellied slider (*Trachemys dorbigni*) and red-footed tortoise *(Chelonoidis carbonarius*) are animals with a large geographic distribution, inhabiting marine, freshwater and terrestrial environments, respectively (RHODIN et al., 2018; KOOLSTRA et al., 2019). The survival of these species is threatened by anthropogenic activities. *T. dorbigni* and *C. carbonarius* are not on the global and regional red lists of endangered species, but *C. mydas* and other species of sea turtle reporte on the Brazilian coast (ICMBio, 2018; CARDOSO-BRITO et al., 2019; IUCN, 2020). Testudines have high visual acuity, and studies on the ophthalmic properties of these animals

highlighted the importance of vision for interacting with the environment and maintaining their survival (NARAZAKI et al., 2013).

The scleral skeleton in the eye of these animals is composed of a bone ring (ossicles) and a cartilage (FRANZ-ODENDAAL & HALL, 2006; PALUMBO et al., 2012; FRANZ-ODENDAAL, 2020). The ring is located at the anterior pole of the eye and although its biological function is poorly understood, it is related to protection against mechanical pressures and the provision of support to maintain the shape, muscle fixation and accommodation of the eye (LIMA et al., 2009; PALUMBO et al., 2012; ZHANG et al., 2012). Studies of anatomical and biometric characteristics of this ring bone, in conjunction with orbit, head and eye biometrics, can provide inferences about activity patterns of these animals, like diurnal or nocturnal behavior (FERNÁNDEZ et al., 2005; HALL, 2008; FRANZ-ODENDAAL, 2020). For Testudines, studies have described the scleral ossicles', developmental pattern and the shape and number of ossicles per ring (FRANZ-ODENDAAL, 2020). Also, some studies provided age estimations based on growth marks on the ossicles (AVENS et al., 2009; AVENS et al., 2020). However, references regarding ocular biometry of those animals are still necessary (MURAMOTO et al., 2020).

In fossil specimens, the morphological characteristics of the scleral ossicle rings are related to the animals' adaptation to aquatic vision (YAMASHITA et al., 2015). ATKINS & FRANZ-ODENDAAL (2016) proved that the morphology, as well as the presence or absence of these rings, are related to the environment and to the behavior of 400 existing species and 19 fossil species of Squamata. However, the lack of publications on the ocular skeleton of the Testudines, especially using diagnostic imaging tools, prevents inferring possible relationships between the anatomy of these structures and a species' ecological niche.

Imaging morphobiometric studies are important for *in vivo* descriptions and have already been used for the anatomical evaluation of celomatic cavity of Testudines (*C. carbonarius*, *Testudo hermanni* and *Trachemys* spp.) (MEIRELES et al., 2016; PAJDAK-CZAUS et al., 2019). Similar analyses have also been performed for endocranial evaluation of fossil Testudines (*Naomichelys speciosa*, *Galianemys emringeri*, *Galianemys whitei*, *Nichollsemys baieri* and *Hamadachelys escuilliei*) and living animals (*Trachemys scripta elegans* and *Malaclemys terrapin*) (WILLIS et al., 2013; PAULINA-CARABAJAL et al., 2019).

Despite the importance of the scleral ossicle ring and the applicability of imaging tests for anatomical descriptions in live animals, comparative studies of the scleral skeleton are not found among the Testudines. Therefore, this study described the main morphobiometric characteristics of the scleral ossicle rings of three specimens of Testudines using non-invasive examinations: ultrasonography (US) and computed tomography (CT).

MATERIALS AND METHODS

Animals

Animals from three Testudines species were evaluated: one green turtle (*C. mydas*), female, juvenile, from the Fundação Projeto Tamar – Praia do Forte, Bahia, Brazil; one black-bellied slider (*T. dorbigni*), undefined sex, juvenile; and one red-footed tortoise (*C. carbonarius*), female, juvenile, both from the Centro de Triagem de Animais Silvestres (CETAS-IBAMA, Salvador, Brazil). All animals were subjected to clinical and periocular evaluation under normal light for gross abnormalities with a 3X binocular magnifying loupe and transilluminator and no signs of disease was observed in any of the study animals. The animals were manually restrained, and body weight and curved carapace length were measured prior to US and CT evaluation.

Before the CT, the animals were subjected to 6 h of food and water fasting. Jugular vein catheterization was performed with a 20G catheter for the *C. mydas*, and a 24G catheter for the *T. dorbigni* and *C. carbonarius*. Then they were administered 10 mg/kg 1% propofol (Diprivan®, Caponago, Monza-Brianza, Italy) intravenously to induce anesthesia. Heart and respiratory rates, electrocardiogram, and cloacal temperature were measured with a multiparameter monitor (Dixtal 2022; Philips, São Paulo, Brazil).

After loss of laryngotracheal and ocular reflexes, as well as signs of myorelaxation, the animals were intubated with a 6.5mm endotracheal tube for the *C. mydas* and with the flexible part of a 20G catheter for the *T. dorbigni* and *C. carbonarius*, due to the lack of viable endotracheal tubes for the glottis diameter of these individuals. All animals were kept intubated to provide 100% oxygen and ventilation, as well as to avoid tracheobronchial aspiration. If signs of anesthetic superficialization were observed, 0.5 mg/kg propofol was administered to reestablish the animal's anesthetic plan and immobility.

US evaluation

A Logiqe® portable ultrasound device (GE

Medical Systems, Wuxi, China) was used, with a linear transducer from 7 to 12 MHz and a preadjusted system for the evaluation of small parts and surface structures, to obtain images in B-mode. To perform the exam, one drop of an anesthetic eye drop (1.0% tetracaine with 0.1% phenylephrine hydrochloride, Anestesico®, Allergan, São Paulo, Brazil) was administered to both eyes. The transducer surface, covered with acoustic ultrasound gel (Carbogel ULT®, São Paulo, Brazil), was gently supported on the eyelid or directly on the corneal surface. Scanning movements were performed to obtain images of each eye in the sagittal, dorsal and oblique planes. The same investigator (CM) performed the exams, to minimize measurement errors.

The main sonographic characteristics (general aspect, echotexture and echogenicity) of each scleral ossicle ring were described. In addition, the thickness and width of each ring were measured on images of the eye taken on a scan plane (sagittal, dorsal or oblique) where the ossicle appeared to be better defined. Thus, the measurement location varied between the medial, lateral, superior and inferior regions. The thickness was taken at the level of the middle third of the scleral ossicle's width, from the anterior to the posterior surface. The width was measured from the corneal margin up to the scleral margin (Figure 1). Anechobiometric assessment was also performed on the axial axis (corneal thickness, depth of the anterior chamber, axial length of the lens, depth of the vitreous chamber and axial globe length), and the width along the equatorial axis of each bulb was measured (Supporting Information, table 1).

The ratio of the mean width of the scleral ossicle ring to the axial globe length (AGL) was calculated for each eye of each individual as x = mean width of the scleral ossicle ring/AGL x 100%, where the value of x corresponds to the percentage of AGL represented by the width of the ossicle ring.

CT evaluation

Images were obtained in the axial plane of the heads (median plane of the eyes) using a CT helical scanner (Asteion™ TSX-021B1, with four-row detector, Toshiba Medical Systems Corporation, Tochigi, Japan), with a rotation time of 1.0 s, voltage of 120 kVp, amperage of 150 mAs and slice thickness of 0.5 mm for *C. mydas* and 0.3 mm for *T. dorbigni* and *C. carbonarius*. Images were acquired in a single moment, without intravenous contrast, in soft tissue filter and bone reconstruction mode, with the animals positioned in ventral recumbence. Images were analyzed in the axial plane of the heads (median plane

of the eyes) and reconstructions were performed in the dorsal, longitudinal (sagittal) and tridimensional planes (Supporting Information, Video 1-3).

For each scleral ossicle ring, general characteristics were described and measured by CT (general aspect, shape, position):
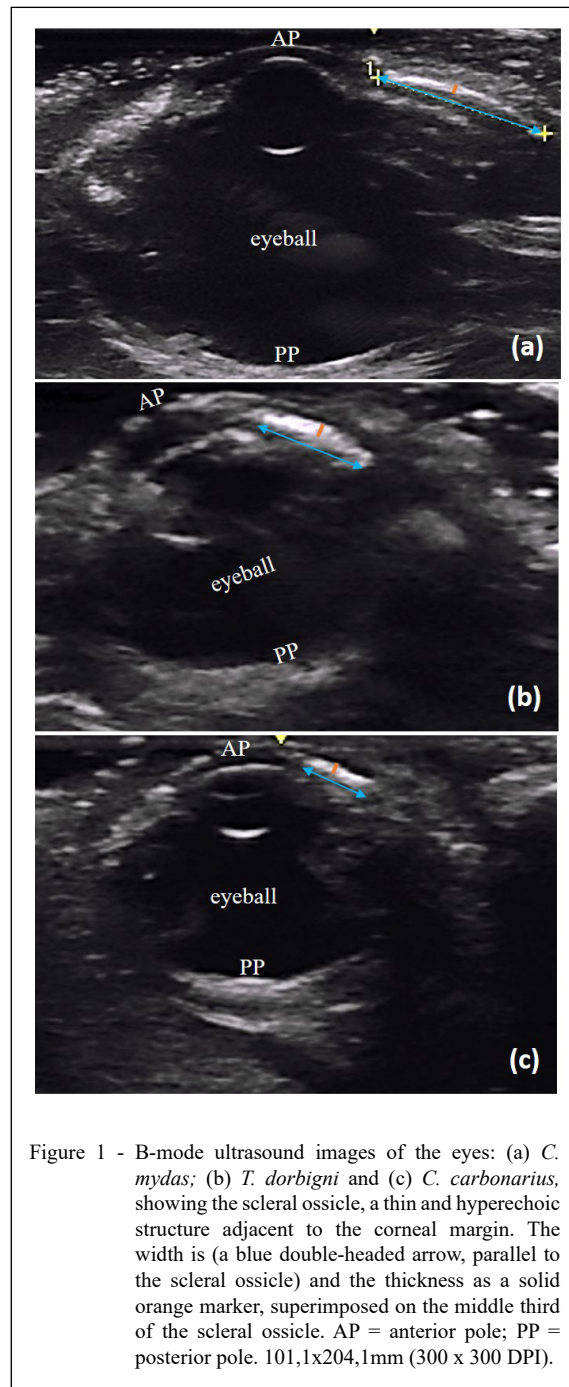a) thickness – in the axial plane of the heads (median plane of the eyes), performed in three regions ranging from the superior to the inferior parts of each ring (close to the corneal margin, in the middle third and close to the scleral margin), from its anterior to the posterior surface;
b) width – measured from the corneal margin up to the scleral margin, in the axial plane of the heads (median plane of the eyes) for the superior and inferior parts of the scleral ring and in the dorsal plane for the medial and lateral parts of the ring;
c) diameters – vertical and horizontal diameters of the outer (posterior, adjacent to the scleral margin) and inner (anterior, adjacent to the corneal margin) scleral ring were measured in an oblique longitudinal (sagittal) reconstruction image;
d) density – in Hounsfield units (HU), in the superior and inferior parts of the scleral ring.

Additional evaluations were performed in the central axial of the heads (median of the eyes) and dorsal planes to obtain the measurements of the segments and the width (in the equatorial axis) of the eye, similar to those performed for the US. Values of the ratio of the width of the scleral ossicle ring to the AGL were also determined, as described for the US measurements.

RESULTS

The US exam revealed the scleral ossicle ring as a single structure, continuous, thin and hyperechoic [bright white on ultrasound]. Both margins, corneal and scleral, of each ossicle ring were located at the anterior pole of the eye, limited by the limbus, around the cornea and under the bulbar conjunctiva, with no connection to any other skull element. The surfaces of the ring, anterior and posterior, were slightly irregular. The *C. mydas* had the largest rings (thickest and widest) and the *C. carbonarius* had the smallest width measurements.

The presence of scleral cartilage was observed only in the green turtle, shaped like a cup located at the posterior part of the eye. The *T. dorbigni* had a longer AGL than the *C. carbonarius*. The proportion of the average width of the scleral ossicle ring to the AGL of each eye corresponded to more than 50% only in the US examination of the green turtle. The

Figure 1 - B-mode ultrasound images of the eyes: (a) *C. mydas;* (b) *T. dorbigni* and (c) *C. carbonarius,* showing the scleral ossicle, a thin and hyperechoic structure adjacent to the corneal margin. The width is (a blue double-headed arrow, parallel to the scleral ossicle) and the thickness as a solid orange marker, superimposed on the middle third of the scleral ossicle. AP = anterior pole; PP = posterior pole. 101,1x204,1mm (300 x 300 DPI).

lowest percentage was found for the *C. carbonarius*. Figure 1 shows the measurements of the ring width in the *C. mydas*, *T. dorbigni* and *C. carbonarius*.

On the CT scans, the shapes and locations of the scleral ossicle rings were similar to that which was observed on the US. The images were sharper on *C. mydas* (Figure 2). *C. mydas* rings had higher thickness values, in all measured regions, than the other two animals. The rings of the *T. dorbigni* showed higher thickness values near the corneal margin and in the middle third than near the scleral margin. For the *C. mydas* and the *C. carbonarius*, a higher thickness value

Table 1 - Biometric data of scleral ossicle rings and eyes of three specimens of Testudines by ultrasound (US) and/or computed tomography (CT).

Measurements		*C.mydas* Weight = 46.2 kg CCL = 78.8 cm				*T.dorbigni* Weight = 0.8 kg CCL = 20.0 cm				*C.carbonarius* Weight = 0.6 kg CCL = 19.3 cm			
		US		CT		US		CT		US		CT		
		RE	LE	RE	LE	RE	LE	RE	LE	RE	LE	RE	LE	
Scleral Ossicle Rings	TS-1 (mm)	-	-	1.1	1.0	-	-	0.7	0.8	-	-	0.6	0.7	
	TS-2 (mm)	-	-	1.1	1.2	-	-	0.7	0.7	-	-	0.7	0.7	
	TS-3 (mm)	-	-	0.7	0.7	-	-	0.6	0.5	-	-	0.5	0.4	
	TI-1 (mm)	-	-	0.8	0.8	-	-	0.6	0.7	-	-	0.7	0.7	
	TI-2 (mm)	-	-	1.1	0.9	-	-	0.6	0.7	-	-	0.7	0.5	
	TI-3 (mm)	-	-	0.9	0.7	-	-	0.5	0.4	-	-	0.5	0.5	
	Thickness[a] (mm)	0.6	0.5	1.1	1.1	0.3	0.4	0.7	0.7	0.4	0.6	0.7	0.6	
	W-1 (mm)	9.2	9.1	9.1	9.7	3.5	4.0	3.3	3.0	2.8	2.7	3.7	4.3	
	W-2 (mm)	10.1	11.0	6.9	6.7	-	-	2.7	2.8	3.6	3.3	2.7	3.0	
	W-3 (mm)	-	-	5.6	5.5	-	-	2.2	2.3	-	-	2.7	2.8	
	W-4 (mm)	-	-	7.5	7.4	-	-	2.5	2.0	-	-	2.8	3.2	
	W-5 (mm)	9.7	10.1	7.3	7.3	3.5	4.0	2.7	2.5	3.2	3.0	3.0	3.3	
	VDOR (mm)	-	-	22.2	21.8	-	-	9.3	9.1	-	-	8.2	8.0	
	HDOR (mm)	-	-	24.2	24.0	-	-	9.2	8.6	-	-	8.3	8.0	
	VDIR (mm)	-	-	10.5	10.5	-	-	7.1	6.4	-	-	4.9	4.9	
	HDIR (mm)	-	-	11.0	11.9	-	-	7.4	7.5	-	-	4.8	5.0	
	D-1 (UH)	-	-	1117-3440	1254-3264			854-1388	636-1009			886-1141	617-1036	
	D-2 (UH)	-	-	1068-2006	1102-2307	-	-	556-1049	505-894			427-679	562-815	
Eyes	AGL (mm)	17.4	17.2	16.9	16.8	8.3	8.3	7.4	7.4	7.8	8.0	7.6	7.9	
	EGW (mm)	25.0	24.8	25.4[ap] 24.2[dp]	24.9[ap] 24.9[dp]	8.7	9.3	8.3[ap] 8.7[dp]	8.3[ap] 8.9[dp]	9.1	9.0	8.5[ap] 9.5[dp]	8.1[ap] 9.1[dp]	
	W/AGL (%)	55.8	58.7	43.3	43.6	42.2	48.2	36.7	33.8	41.0	37.5	39.5	41.8	

CCL = curved carapace length; RE = right eye; LE = left eye; mm = millimeter; HU = Hounsfield units; % = percent; [ap] = axial plane; [dp] = dorsal plane.

Thickness of the superior (TS-1, 2, 3) and inferior (TI-1, 2, 3) regions; width (W-1, 2, 3, 4, 5); vertical and horizontal diameters of the outer ring (VDOR; HDOR) and inner ring (VDIR; HDIR); density (D-1, 2); axial globe length (AGL); equatorial globe width (EGW) and the ratio of width (W-5) to AGL (W/AGL) were displayed.

TS = Thickness of superior part (TS-1, near corneal margin; TS-2, in the middle third; TS-3, near scleral margin).

TI = Thickness of inferior part (TI-1, near the corneal margin; TI-2, in the middle third; TI-3, near scleral margin).

[a]: In US, it corresponds to a single measure in the middle third of where the ossicle appeared to be better defined; In CT, arithmetic mean of the measurements made in the middle thirds of the superior and inferior parts of each scleral ossicle ring was considered.

W = Width measured from the corneal margin up to the scleral margin. For US, width measured where the ossicle appeared to be better defined (W1; W2). For CT, width measured at the superior (W-1), inferior (W-2), medial (W-3) and lateral (W-4) parts of each ring. W-5 = arithmetic mean of the widths measured in US and CT.

VDOR= Vertical diameter of the outer ring; HDOR = Horizontal diameter of the outer ring.

VDIR = Vertical diameter of the inner ring; HDIR = Horizontal diameter of the inner ring.

D = Density of superior (D-1) and inferior (D-2) regions of the scleral rings (HU).

AGL =Axial globe lenght, obtained from the arithmetic mean of measurements taken on axial and dorsal planes, from the anterior surface of the cornea to the eye fundus.

EGW = Equatorial globe width (approximated values).

W/AGL: The ratio of the mean width (W) of the scleral ossicle ring to the AGL.

was only observed in the superior part of the rings. Mean thickness values were similar for the *T. dorbigni* and *C. carbonarius*. The width of the measured regions was greatest for the *C. mydas* rings, and lowest for the *T. dorbigni* rings. The horizontal diameters were larger than the vertical diameters for the *C. mydas*, at each of the outer and inner ring. However, for the *T. dorbigni*, this only happened in the rings' inner diameter.
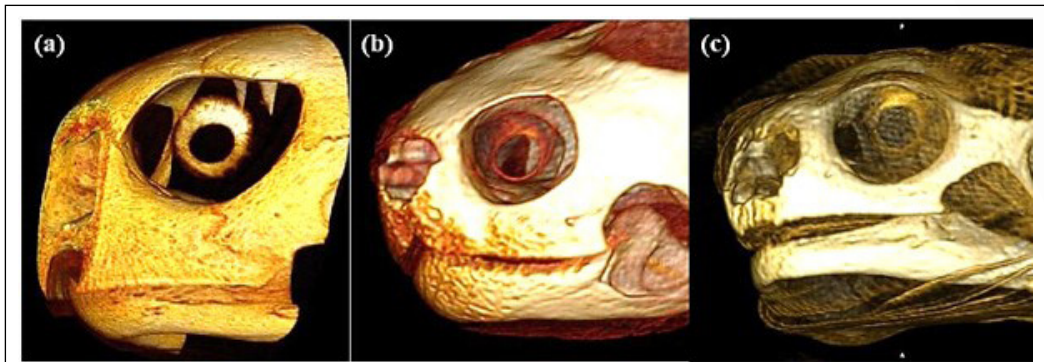
Figure 2 - Computed tomography image in three-dimensional reconstruction of the scleral ossicle rings: (a) *C. mydas* with better image than in (b) *T. dorbigni*, which the image sharpness was lower and (c) *C. carbonarius*. 159,8 x 54,7mm (300 x 300 DPI).

Densitometric analysis revealed lowest ossicle density in the *C. carbonarius* and the highest density in the *C. mydas*. For the three animals, the density at the superior part was higher than at the inferior of each ossicle ring. Figure 3 shows some measurements of the scleral ossicle ring of the three animals.

On the CT images, scleral cartilage was only observed in the *C. mydas*, with a shape and location similar to that described in the US. The proportion of the width of the scleral ossicle ring to the AGL of each eye was also greater in the *C. mydas*, as with the US, whenever the AGL was observed without considering the presence of scleral cartilage. However, no proportion was greater than or equal to 50%. All biometric CT values are shown in table 1, displayed so that they can be compared to the US results. After performing the CT exam, each animal was kept under observation until full recovery.
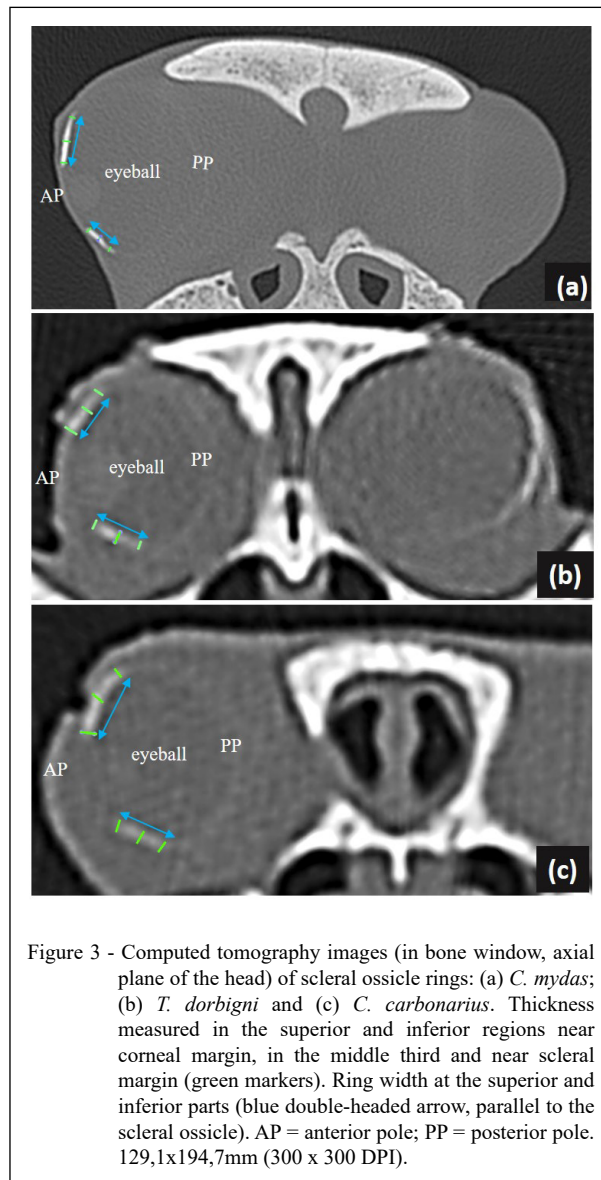
DISCUSSION

Non-invasive imaging exams (US and CT) were performed to describe scleral ossicle rings in three live species of Testudines. These diagnostic techniques have proven useful in the study of reptile anatomy (PAJDAK-CZAUS et al., 2019; PAULINA-CARABAJAL et al., 2019). The morphological knowledge of associated ocular structures is fundamental for ophthalmology and is important for the distinction between taxa, age estimation and activity patterns of animals – once there is a close relationship between eye and orbit dimensions, and between these and scotopic or photopic activities of species (FERNÁNDEZ et al., 2005; OLIVEIRA et

al., 2008; SCHMITZ & MOTANI, 2011).

The scleral ossicle rings of the three animals belonging to the same taxonomic order presented similar forms. Differences in the shape of the rings, described in birds, are the consequence of thousands of years of evolution; however, similar morphological patterns in species of the same order are maintained (LIMA et al., 2009; FRANZ-ODENDAAL, 2020). The circular and continuous appearance of each ring, seen in the images as a single structure and without adjacent sesamoids, differed from the morphological descriptions in some osteotechnical studies, such as diaphanization and staining with Alizarin red, or in microscopic analyses (such as stereomicroscopy, confocal laser-scanning microscopy and energy-dispersion spectroscopy). Those studies described this structure as a framework composed of 8 to 18 individual and overlapping trapezoids ossicles (ZHANG et al., 2012; FRANZ-ODENDAAL, 2020). FRANZ-ODENDAAL & VICKARYOUS (2006), discussed the development and distribution of the eye's skeletal elements and mentioned the presence of sesamoids in scleral rings of snake, crocodilian and some nocturnal birds. In the current study, and having similar locations in the three animals, all rings were positioned with no connection to other skull elements, in agreement with other studies (ZHANG et al., 2012; FRANZ-ODENDAAL, 2020).

The assessment of the irregularities observed by US in the faces of the scleral ossicle rings on the three animals may suggest that those are sites for muscle fixation, but we can not affirm. YAMASHITA et al. (2015) also reported irregularities in the posterior face of the scleral rings in reptiles

Figure 3 - Computed tomography images (in bone window, axial plane of the head) of scleral ossicle rings: (a) *C. mydas*; (b) *T. dorbigni* and (c) *C. carbonarius*. Thickness measured in the superior and inferior regions near corneal margin, in the middle third and near scleral margin (green markers). Ring width at the superior and inferior parts (blue double-headed arrow, parallel to the scleral ossicle). AP = anterior pole; PP = posterior pole. 129,1x194,7mm (300 x 300 DPI).

from the Mosossauridae family. To these authors, those areas may serve as muscle fixation places. In a review about skeletal elements of vertebrates' eyes, FRANZ-ODENDAAL & VICKARYOUS (2006) observed that the presence of a scleral sesamoid bone in some reptiles (e.g. snakes and crocodiles) and nocturnal birds may serve to act as anchor for the pyramidal nictitating muscle and prevent its tendon from being projected over the cornea.

Our CT evaluation revealed that the scleral ossicle rings in all animals were thicker near the corneal margin and in the middle third, than along the scleral margin. YAMASHITA et al. (2015) also reported this characteristic in their study with five fossil specimens of mosasaurs. However, the limited number of animals in our study prevents us from attributing this finding to Testudines in general.

The greater thickness reported for the *C. mydas*'s scleral rings, especially in their superior parts, might be due to the influence of water pressure on the eyes during diving, or air pressure, the latter producing thicker scleral bones in fast-flying birds, for instance (FRANZ-ODENDAAL, 2008). Sea turtles are known to spend much of their time diving: they stay submerged for long periods and then emerge briefly and dive again (HAYS et al., 2000; BALDINI

et al., 2019); however, studies with scope are needed to directly assess the influence of water pressure on the thickness of the ossicle rings.

As reported by YAMASHITA et al. (2015) in mosasaur fossils, the scleral rings were wider in their superior region than in their inferior. The eye size was considered positively correlated with the bone orbit size and with mammalian visual acuity (FERNÁNDEZ et al., 2005; VEILLEUX & KIRK, 2014). OLLONEN et al. (2018) studied orbits that occupy a great portion of the skull (almost one third) on the adult central bearded dragon (*Pogona vitticeps*), animals whose eyes were considered relatively big. The definition of those orbital parameters is useful for ophthalmology once the orbital affections may exist when exophthalmetric values are out of the normal range (CHAN et al., 2009).

Even qualitatively, the measurements of scleral ossicle rings are significant to the estimation of cornea and eye bulb size, ophthalmic structures that are intimately related to the vision ability and lifestyle (FERNÁNDEZ et al., 2005). Therefore, if the width (size) of the ossicle ring is proportional to the AGL, and the AGL of the Testudines in this study classifies them as short-eyed animals (AGL <22.0 mm) according to ophthalmic medicine (DAY et al., 2012; CARIFI et al.,2015; DONG et al., 2018), a question can be raised as to the level of visual acuity in these species.

The internal diameter of the scleral ossicle ring provides an estimate of cornea (and pupil) size, which can be used to infer the amount of light that can potentially enter the eye, and to assist in determining the animal's pattern of activity (FRANZ-ODENDAAL, 2020). In our study, the vertical and horizontal diameters of the outer and inner ring were greatest for the *C. mydas* specimen. The internal diameters of the rings for the *T. dorbigni* were larger than those for the *C. carbonarius*, possibly explaining why the former's rings were less wide. On a paleontological study with Ichthyosaurian fossils the internal area of the ring represented 20% of the orbital area (FERNÁNDEZ et al., 2005**)**.

Variation in bone density values recorded for the scleral ossicle ring, from the lowest value in the *C. carbonarius* to the highest value in the *C. mydas*, does not allow an analysis of the normality pattern. Although bone densities have been reported for reptiles (turtles, snakes and lizards), these were evaluations of pleural and neural bones and dorsal vertebrae, as well as differences between compact and trabecular bones (GUMPENBERGER, 2011; ARAÚJO et al., 2019); as such, there are still no densitometric reference values for scleral rings.

In this study, scleral cartilage was seen only in the *C. mydas* eye. FRANZ-ODENDAAL & HALL

(2006) reported the presence of scleral cartilage in the eyes of diaphanized embryos of snapping turtle (*Chelydra serpentina*). The shape and condition of the cartilage observed in the *C. mydas* were in accordance with descriptions for reptiles (BRUDENALL et al., 2008; FRANZ-ODENDAAL, 2020). The presence of hard structures that support the eye may be an indication of the influence of ecological niche on anatomy (HALL, 2008; FRANZ-ODENDAAL, 2020). However, studies on scleral cartilage are scarce, and further research on this topic is warranted.

US and CT proved to be good tools for the morphobiometric study of the scleral ossicle rings of three Testudines species. US has been shown to be safe because it does not require the use of ionizing radiation, and CT's advantage lies in its greater precision for bones and adjacent structures (BALDINI et al., 2019). However, for studies aiming to describe the individual ossicles that overlap to form each scleral ring, the use of tools with higher image resolution is recommended, such as the micro-CT (BAKAR et al., 2019; LANTYER-ARAÚJO et al., 2019).

CONCLUSION

The *C. mydas*, *T. dorbigni* and *C.carbonarius* specimens are morphologically similar with respect to the shape and location of their scleral ossicle rings. However, the *C. mydas* rings had the largest biometric dimensions. This is the first report on anatomical knowledge obtained by imaging Testudines scleral ossicle rings and can serve as a basis for the design of future studies.

The US and CT proved to be good non-invasive tools to study the anatomy of the ocular skeleton in live Testudines. CT allows a greater number of scleral ossicle ring evaluations.

ACKNOWLEDGEMENTS

DECLARATION OF CONFLICT OF INTEREST

All authors declare that they do not have any

AUTHORS' CONTRIBUTIONS

All authors contributed equally for the conception and writing of the manuscript. All authors critically revised the manuscript and approved of the final version.

BIOETHICS AND BIOSSECURITY COMMITTEE APPROVAL

Ethical approval was obtained by the Ethics Committee for the Use of Experimental Animals of the School of Veterinary Medicine and Zootechny, Universidade Federal da Bahia (protocol no. 36/2015). The research was performed in accordance with the Authorization and Information System of Biodiversity, Brazilian Ministry of the Environment–SISBIO (process nos. 27489 and 50054).

REFERENCES

ARAÚJO, G. G. A. S. et al. Osteodensitometry and tomographic findings in four captive giant South American turtles (*Podocnemis expansa*) with metabolic bone disease. **Journal of Zoo and Wildlife Medicine**, v.50, n.2, p.447–452, 2019. Available from: <https://doi.org/10.1638/2018-0126>. Accessed: Oct. 17, 2020. doi: 10.1638/2018-0126.

ATKINS, J. B.; FRANZ-ODENDAAL, T. A. The sclerotic ring of squamates: an evo-devo-eco perspective. **Journal of Anatomy**, v.229, n.4, p.503–513, 2016. Available from: <https://doi.org/10.1111/joa.12498>. Accessed: May, 17, 2021. doi: 10.1111/joa.12498.

AVENS, L. et al. Use of skeleton chronological analysis to estimate the age of leatherback sea turtles *Dermochelys coriacea* in the western North Atlantic. **Endangered Species Research**, v.8, n.3, p.165–177, 2009. Available from: <https://doi.org/10.3354/esr00202>. Accessed: May, 17, 2021. doi: 10.3354/esr00202.

AVENS, L. et al. Regional comparison of leatherback sea turtle maturation attributes and reproductive longevity. **Marine Biology**, v.167, n.4, p.12, 2020. Available from: <https://doi-org.ez10.periodicos.capes.gov.br/10.1007/s00227-019-3617-y>. Accessed: May, 16, 2021. doi: 10.1007/s00227-019-3617-y.

BALDINI, M. et al. Ultrasound examination of coelomic viscera through the plastron in stranded green sea turtles (*Chelonia mydas*). **Open Veterinary Journal**, v.9, p.38–43, 2019. Available from: <https://dx.doi.org/10.4314/ovj.v9i1.7>. Accessed: Oct. 16, 2020. doi: 10.4314/ovj.v9i1.7.

BAKAR, N. N. A. et al. Measurement of trabecular bone parameters with different bone thicknesses and voxel sizes in mice using micro-CT. **Malaysian Journal of Fundamental and Applied Sciences**, v.15, n.1, p.65–68, 2019. Available from: <https://doi.org/10.11113/mjfas.v15n2019.1128>. Accessed: Oct. 16, 2020. doi: 10.11113/mjfas.v15n2019.1128.

BRUDENALL, D. K. et al. Ocular morphology of the Leatherback sea turtle (*Dermochelys coriacea*). **Veterinary Ophthalmology**, v.11, n.2, p.99–110, 2008. Available from: <https://doi.org/10.1111/j.1463-5224.2008.00607.x>. Accessed: Oct. 16, 2020. doi: 10.1111/j.1463-5224.2008.00607.x.

CARDOSO-BRITO, V. et al. Conjunctival bacterial flora and antimicrobial susceptibility of captive and free-living sea turtles in Brazil. **Veterinary Ophtalmology**, v.22, p.246–255, 2019. Available from: <https://doi.org/10.1111/vop.12584>. Accessed: May, 16, 2021. doi: 10.1111/vop.12584.

CARIFI, G. et al. Accuracy of the refractive prediction determined by multiple currently available intraocular lens power calculation formulas in small eyes. **American Journal of Ophthalmology**, v.159, n.3, p.577-583, 2015. Available from: <https://doi.org/10.1016/j.ajo.2014.11.036>. Accessed: May, 20, 2021. doi: 10.1016/j.ajo.2014.11.036.

CHAN, W. et al. Exophthalmometric values and their biometric correlates: The Kandy Eye Study. **Clinical & Experimental Ophthalmology**, v.37, p.496-502, 2009. Available from: <https://doi.org/10.1111/j.1442-9071.2009.02087.x>. Accessed: May, 20, 2020. doi: 10.1111/j.1442-9071.2009.02087.x.

DAY, A. et al. Accuracy of intraocular lens power calculations in eyes with axial length <22.00mm. **Clinical & Experimental Ophthalmology**, v.40, n.9, p.855-862, 2012. Available from: <https://doi.org/10.1111/j.1442-9071.2012.02810.x>. Accessed: May, 20, 2020. doi: 10.1111/j.1442-9071.2012.02810.x.

DONG, J. et al. Comparison of axial length, anterior chamber depth and intraocular lens power between IOL Master and ultrasound in normal, long and short eyes. **PLoS One**, v.13, n.3, e0194273, 2018. Available from: <https://doi.org/10.1371/journal.pone.0194273>. Accessed: Oct. 18, 2020. doi: 10.1371/journal.pone.0194273.

FERNÁNDEZ, M.S. et al. Ichthyosaurian eyes: paleobiological information content in the sclerotic ring of C*aypullis aurus* (Ichthyosauria, Ophthalmosauria). **Journal of Vertebrate Paleontology**, v.25, p.330-337, 2005. Available from: <https://doi-org.ez10.periodicos.capes.gov.br/10.1671/0272-4634>. Accessed: Oct. 18, 2020. doi: 10.1671/0272-4634.

FRANZ-ODENDAAL, T. A.; HALL, B. K. Skeletal elements within teleost eyes and a discussion of their homology. **Journal of Morphology**, v.267, p.1326–1337,2006. Available from: <https://doi.org/10.1002/jmor.10479>. Accessed: Oct. 18, 2020. doi: 10.1002/jmor.10479.

FRANZ-ODENDAAL, T. A.; VICKARYOUS, M. K. Skeletal Elements in the Vertebrate Eye and Adnexa: Morphological and Developmental Perspectives. **Developmental Dynamics**, v.235, p.1244 –1255, 2006. Available from: <https://doi.org/10.1002/dvdy.20718>. Accessed: May, 20, 2020. doi: 10.1002/dvdy.20718.

FRANZ-ODENDAAL, T. A. Scleral ossicles of Teleostei: evolutionary and developmental trends. **The Anatomical Record**, v.291, p.161–168, 2008. Available from: <https://doi.org/10.1002/ar.20639>. Accessed: May, 20, 2021. doi: 10.1002/ar.20639.

FRANZ-ODENDAAL, T. A. Skeletons of the eye: an evolutionary and developmental perspective. **The Anatomical Record**, v.303, p.100–109, 2020. Available from: <https://doi.org/10.1002/ar.24043>. Accessed: Oct. 17, 2020. doi: 10.1002/ar.24043.

GUMPENBERGER, M. Chelonians. In: SCHWARZ, T.; SAUNDERS, J. **Veterinary Computed Tomography**. Oxford:

Wiley-Blackwell, 2011. Chap.50, p.533–544.

HALL, M. I. The anatomical relationships between the avian eye, orbit and sclerotic ring: implications for inferring activity patterns in extinct birds. **Journal of Anatomy**, v.212, p.781–794, 2008. Available from: <https://doi.org/10.1111/j.1469-7580.2008.00897.x>. Accessed: Oct. 18, 2020. doi: 10.1002/ar.24043.

HAYS, G. C. et al. Diving behaviour of green turtles: dive depth, dive duration and activity levels. **Marine Ecology Progress Series**, v.208, p.297–298, 2000. Available from: <https://doi.org/10.3354/meps208297>. Accessed: Oct. 18, 2020. doi: 10.3354/meps208297.

ICMBio - INSTITUTO CHICO MENDES DE CONSERVAÇÃO DA BIODIVERSIDADE. **Livro Vermelho da Fauna Brasileira Ameaçada de Extinção**, v I / -- 1 ed., 492 p. -- Brasília, DF: ICMBio/MMA, 2018. Available from: <https://www.icmbio.gov.br/portal/images/stories/comunicacao/publicacoes/publicacoes-diversas/livro_vermelho_2018_vol1.pdf>. Accessed: May, 18, 2021.

IUCN - International Union for Conservation of Nature. **Red List of Threatened Species**. Available from: <https://www.iucnredlist.org>. Accessed: Oct. 15, 2020.

KOOLSTRA, F. J. et al. Comparative osteology and osteometry of the coracoideum, humerus, and femur of the green turtle (*Chelonia mydas*) and the loggerhead turtle (*Caretta caretta*). **International Journal of Osteoarchaeology**, v.29, p.683–695, 2019. Available from: <https://doi-org.ez10.periodicos.capes.gov.br/10.1002/oa.2761>. Accessed: May, 16, 2021. doi: 10.1002/oa.2761.

LANTYER-ARAÚJO, N. L. et al. Anatomical, histological and computed tomography comparisons of the eye and adnexa of crab-eating fox (*Cerdocyon thous*) to domestic dogs. **PLoS One**, v.14, n.10, e0224245, 2019. Available from: <https://doi.org/10.1371/journal.pone.0224245>. Accessed: Oct. 16, 2020. doi: 10.1371/journal.pone.0224245.

LIMA, F. C. et al. Anatomy of the scleral ossicles in Brazilian birds. **Brazilian Journal of Morphological Sciences**, v.26, n.3-4, p.165–169, 2009. Available from: <http://www.jms.periodikos.com.br/article/587cb4907f8c9d0d058b474a/pdf/>>. Accessed: Oct. 16, 2020.

MEIRELES, Y. S. et al. Ultrasound characterization of the coelomic cavity organs of the red-footed tortoise (*Chelonoidis carbonaria*). **Ciência Rural**, v.46, n.10, p.1811–1817, 2016. Available from: <https://dx.doi.org/10.1590/0103-8478cr20150876>. Accessed: May, 17, 2021. doi: 10.1590/0103-8478cr20150876.

MURAMOTO, C. et al. Ocular ultrasonography of sea turtles. **Acta Veterinaria Scandinavica**, v.62, n.1, p.52, 2020. Available from: <https://doi.org/10.1186/s13028-020-00551-1>. Accessed: May, 16, 2021. doi: 10.1186/s13028-020-00551-1.

NARAZAKI, T. et al. Loggerhead turtles (*Caretta caretta*) use vision to forage on gelatinous prey in mid-water. **PLoS One**, v.8, n.6, e66043, 2013. Available from: <https://doi.org/10.1371/journal.pone.0066043>. Accessed: Oct. 15, 2020. doi: 10.1371/journal.pone.0066043.

OLIVEIRA, L. R. et al. Morphological and genetic evidence for two evolutionarily significant units (ESUs) in the South American fur seal, *Arctocephalus australis*. **Conservation Genetics**, v.9, p.1451–1466, 2008. Available from: <https://doi.org/10.1007/s10592-007-9473-1>. Accessed: May, 20, 2020. doi: 10.1007/s10592-007-9473-1.

OLLONEN, J. et al. Skull Development, Ossification Pattern, and Adult Shape in the Emerging Lizard Model Organism *Pogona vitticeps*: A Comparative Analysis With Other Squamates. **Frontiers in Physiology**, v.9, n.28, p.278, 2018. Available from: <https://doi.org/10.3389/fphys.2018.00278>. Accessed: May, 20, 2020. doi: 10.3389/fphys.2018.00278.

PALUMBO, C. et al. Osteocyte apoptosis and absence of bone remodeling in human auditory ossicles and scleral ossicles of lower vertebrates: a mere coincidence or linked processes? **Calcified Tissue International**, v.90, p.211–218, 2012. Available from: <https://doi.org/10.1007/s00223-012-9569-6>. Accessed: Jun. 10, 2020. doi: 10.1007/s00223-012-9569-6.

PAJDAK-CZAUS, J. et al. Applicability of thyroxine measurements and ultrasound imaging in evaluations of thyroid function in turtles. **Journal of Veterinary Research**, v.63, n.2, p.267–273, 2019. Available from: <https://doi.org/10.2478/jvetres-2019-0029>. Accessed: Jun. 17, 2020. doi: 10.2478/jvetres-2019-0029.

PAULINA-CARABAJAL, A. et al. The endocranial anatomy of the stem turtle *Naomichelys speciosa* from the Early Cretaceous of North America. **Acta Palaeontologica Polonica**, v.64, n.4, p.711–716, 2019. Available from: <https://doi.org/10.4202/app.00606.2019>. Accessed: Jun. 17, 2020. doi: 10.4202/app.00606.2019.

RHODIN, A. G. J. et al. Global Conservation Status of Turtles and Tortoises (Order Testudines). **Chelonian Conservation and Biology**, v.17, n.2, p.135-161, 2018. Available from: <https://doi.org/10.2744/CCB-1348.1>. Accessed: May, 16, 2021. doi: 10.2744/CCB-1348.1.

SCHMITZ, L.; MOTANI, R. Nocturnality in dinosaurs inferred from scleral ring and orbit morphology. **Science**, v.332, n.6030, p.705–708, 2011. Available from: <https://doi.org/10.1126/science.1200043>. Accessed: May, 20, 2021. doi: 10.1126/science.1200043.

VEILLEUX, C. C.; KIRK, E. C. Visual acuity in mammals: effects of eye size and ecology. **Brain, Behavior and Evolution**, v.83, n.1, p.43–53, 2014. Available from: <https://doi.org/10.1159/000357830>. Accessed: Oct. 20, 2020. doi: 10.1159/000357830.

WILLIS, K. L. et al. Middle ear cavity morphology is consistent with an aquatic origin for Testudines. **PLoS One**, v.8, n.1, e54086, 2013. Available from: <http://nrs.harvard.edu/urn-3:HUL.InstRepos:10872802>. Accessed: May, 17, 2021. doi: 10.1371/journal.pone.0054086.

YAMASHITA, M. et al. Sclerotic rings in mosasaurs (Squamata: Mosasauridae): structures and taxonomic diversity. **PLoS One**, v.10, n.2, e0117079, 2015. Available from: <https://doi.org/10.1371/journal.pone.0117079>. Accessed: Oct. 17, 2020. doi: 0.1371/journal.pone.0117079.

ZHANG, G. et al. Development and mineralization of embryonic avian scleral ossicles. **Molecular Vision**, v.18, p.348–361, 2012. Available from: <http://www.molvis.org/molvis/v18/a38>.